

End to End Simulations of Gravitational Wave Electromagnetic Follow-Up Program

Jonathan Ward

*Department of Physics and Astronomy,
Ursinus College, Collegeville, Pennsylvania*

August 14, 2012

Abstract

The search for gravitational waves is about to enter a new scientific era. The expected completion of Advanced Ligo and Advanced Virgo in the coming years will provide physicists with the necessary tools to achieve the first direct detection of gravitational waves. The likely sources of GWs are catastrophic astrophysical events, such as supernova and binary mergers. In addition to gravitational radiation, these events emit large amounts of electromagnetic radiation. These signals, in the form of gamma ray bursts, x-rays, and visible light, can be observed from earth using one or more of the many advanced telescopes stationed all over the world. A joint gravitational wave and electromagnetic observation from a single source would yield rich scientific results. The ability of a telescope to respond to a gravitational wave alert at any given time depends on many factors including sun location, moon location, moon illumination, position of the GW source in the sky and it's magnitude, weather, and the elapsed time since the astrophysical event occurred. All of these factors are tied together in a master simulation that determines an overall "yes" or "no" for the observation of a GW source by a given telescope. Preliminary results are obtained for the TAROT South telescope to determine the probability that a successful observation can be achieved. The capabilities of this simulation are just beginning to be explored, but the hope is to use these simulations to develop the most efficient worldwide telescope network for conducting follow up observations of gravitational wave detections.

1 Gravitational Radiation

1.1 Spacetime

Spacetime is the mathematical model that physicists use to tie space and time together into a single entity that exists everywhere in the universe. Spacetime becomes distorted

in the vicinity of extremely massive objects such as planets, stars, and black holes. A common analogy used to visualize spacetime in the neighborhood of a massive object is the "bowling ball on a rubber sheet" idea. If the sheet is undisturbed with no mass laid on it, it will remain flat. However, placing a

large object, such as a bowling ball, at the center of the sheet will cause it to dip in the middle with the largest displacement from its original position coming directly beneath the center of mass of the bowling ball. Although this may not be exactly what is going on in reality, it is a good way to visualize the key ideas of how spacetime responds to a massive object.

1.2 Gravitational Waves

Imagine that the bowling ball simply sits there. The dip in the middle of the sheet remains, but the system as a whole is basically undisturbed. Now imagine that the bowling ball suddenly begins to move violently, or it is blown up by an explosive at its center. Even if the sheet is extremely large, observers at the far ends of the sheet would still detect ripples or vibrations from the violently moving ball that propagate through the rubber medium. This is the basic idea of gravitational waves. Huge astrophysical events create ripples in spacetime that carry energy in the form of gravitational radiation and propagate in all directions away from the source. The existence of this gravitational radiation is predicted by Albert Einstein in his theory of General Relativity.

1.3 LIGO and VIRGO

LIGO and VIRGO are advanced interferometers that have been built to measure the effect of gravitational waves on spacetime. Both are currently being modified into ALIGO and AVIRGO, which are expected to be ten times more sensitive than the originals and will most likely lead to the first direct detection of gravitational waves. A

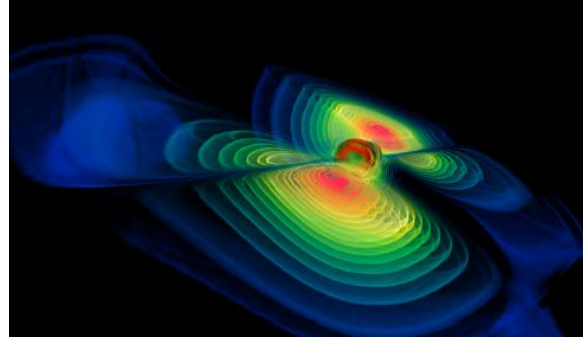


Figure 1: A computer simulation of the gravitational radiation produced by two colliding black holes. The strength of the wave dissipates as it moves further away from the source, similar to that of ripples in a pond.[5]

simplified schematic diagram of LIGO can be seen in Figure 2. The effect of a passing

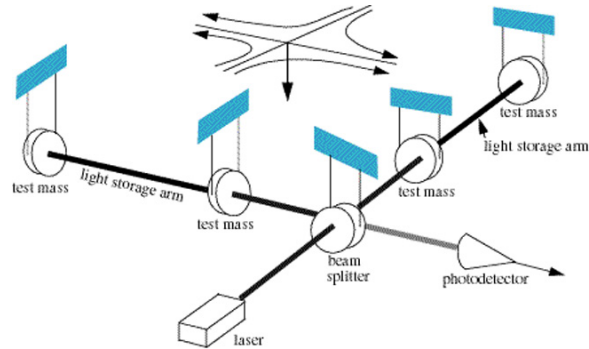


Figure 2: Simplistic experimental setup of LIGO. The 4 km arms are flagged in blue.[2]

gravitational wave on spacetime can be seen in Figure 3. If the wave passes along a line perpendicular to the face of a ring of stationary particles, they will oscillate as shown. When applied to LIGO and VIRGO, a gravitational wave will stretch one arm of the interferometer and shorten the other. Figure 3 is exaggerated to show how the particles respond to a passing wave. In reality the

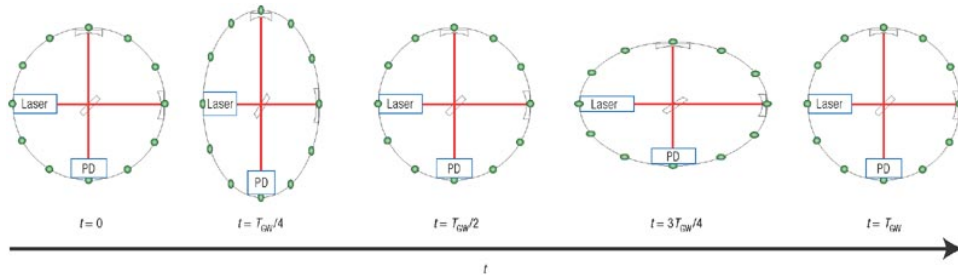


Figure 3: The effect of a passing gravitational wave on a ring of stationary particles. The wave is incident perpendicular to the face of the ring. The ring is transposed on a diagram of a simple interferometer to understand how this mechanism can be used to detect a passing wave. As the wave passes through the face of the circle, the first oscillation stretches the vertical arm and shrinks the horizontal arm and the second oscillation does the opposite.[11]

change in length of an arm will be on the order of 10^{-18} meters.[1] This change in distance is detected by the extremely sensitive lasers in the arms of the interferometer and thus a passing wave can be identified.

expected from the immediate neighborhood of a GRB central engine.[8] There are two types of gamma ray bursts, long (>2 seconds) and short (<2 seconds). Long

2 Electromagnetic Radiation

In addition to gravitational radiation, astrophysical events also emit electromagnetic radiation. There are many forms of this, including visible light, x rays, and gamma rays. Supernovas can be so powerful and so giant that they can be visible to the naked eye for weeks or even months after it occurs. Optical observations of astrophysical events have been possible for decades and it is an extremely reliable method for following up possible gravitational wave detections.

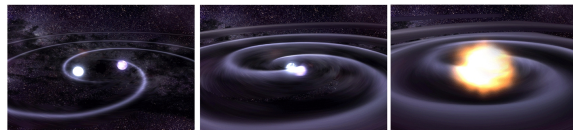


Figure 4: The source of short GRBs, a binary inspiral. These binary mergers come in many forms including NS-NS, NS-BH, and BH-BH.[12]

2.1 Gamma Ray Bursts

Gamma ray bursts are the electromagnetic result of catastrophic and violent astrophysical events. Gravitational radiation can be

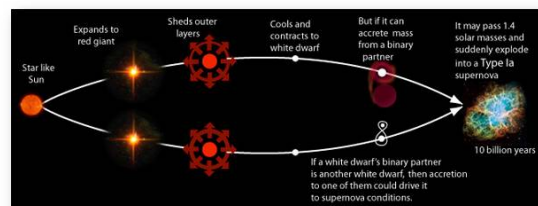


Figure 5: The source of long GRBs, a supernova. "Afterglows" from supernova can be detected hours after the event occurs.[14]

GRBs come from events such as supernova, whereas short GRBs are typical of binary

mergers. Both types of events are prime candidates for producing gravitational waves strong enough to be detected on earth.

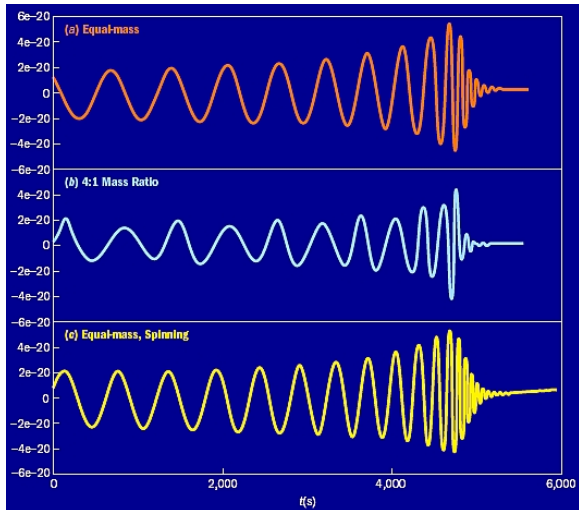


Figure 6: Simulated gravitational wave signals from a binary merger. The frequency and amplitude of the signal increase as the two objects inspiral towards each other. The point of maximum amplitude and frequency corresponds to the final collision of the two objects.[6]

3 Joint GW/EM Observations

3.1 Wave Detection Verification

The detection of a gravitational wave by one interferometer will not be enough evidence to declare that a wave has been successfully observed. A confirmed detection will most likely require matching data from a partner interferometer. It is highly unlikely that noise or anything other than a gravitational wave will produce like data sets at matching times at detectors located across the world from each other. The only other method

that may verify a single gravitational wave detection would be to obtain a corresponding electromagnetic follow up observation. Based on data that can be gathered from each individual observation, such as time, location of source, distance, and magnitude, the two observations can be compared and linked. This would certainly provide the necessary evidence to declare that the detection was in fact a gravitational wave rather than noise or some other fault in the data.

3.2 Scientific Benefits

A joint electromagnetic/gravitational wave observation would yield rich scientific results. Observing the universe through the electromagnetic spectrum has provided answers to many scientific questions, and the ability to do the same through the gravitational wave spectrum is predicted to add many more capabilities. The details of the following will not be discussed, as they are beyond the scope and point of this paper, but benefits of joint EM/GW observations include: The uncertainty in the source position will be reduced from degrees to arc seconds. Also a direct measurement of the local Hubble constant will be possible. Finally, the predictions of General Relativity dealing with gravitational waves have not been tested yet due to the fact that an actual wave has yet to be detected. Joint observations could be used to verify many untested predictions of GR such as propagation speeds and polarizations of gravitational waves.[13] These are only a few of the many doors that a joint GW/EM observation will open for the scientific community.

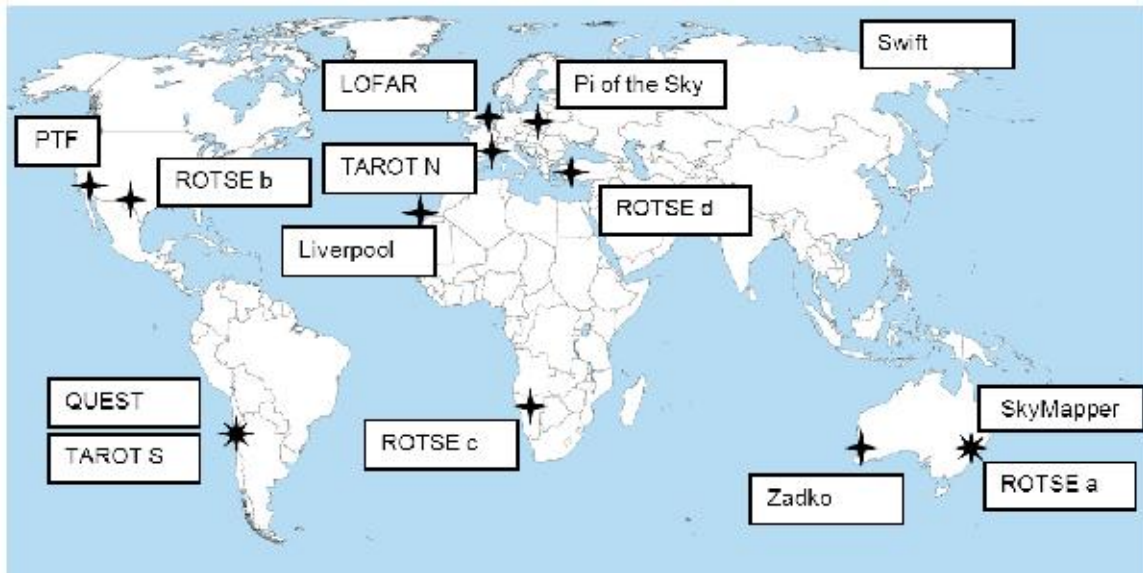


Figure 7: Global telescope network used in the first electromagnetic follow-up program conducted during previous LIGO and VIRGO experimental periods. These telescopes will be used in the first runs of the simulation.[13]

3.3 Difficulties

Although the overall concept is simple, achieving joint GW/EM observations tend to be extremely difficult. The location of a gravitational wave source as provided by the GW signal is not very precise and a single telescope can only view a very small fraction of the sky at a given time. Many conditions must be met in order for a telescope to be able to observe a GW source, or any object in the sky for that matter. In addition to locating the source, it must be dark enough, the weather must be clear, and the source must be observable. The interference of the Moon also comes into play, as well as the inherent characteristics of the telescope, such as field of view and aperture. For these reasons, it would be foolish to rely on a single telescope as the sole response sys-

tem to gravitational wave alerts. The maximum possible sky coverage is needed and the participating telescopes must be in locations that maintain ideal observation conditions during the experimental runs. Thus a global network of strategically placed telescopes is needed to optimize the chances of a joint observation. Figure 6 shows an example network that was used in the follow up program during the last active experiments conducted by LIGO and VIRGO. This network is a good starting point, but it is necessary to answer key questions before launching such a vast project. How many telescopes are needed? What should their field of view and aperture be? Where should they be located? A simulation has been developed to answer these and other questions that will identify the best possible electromagnetic follow up system.

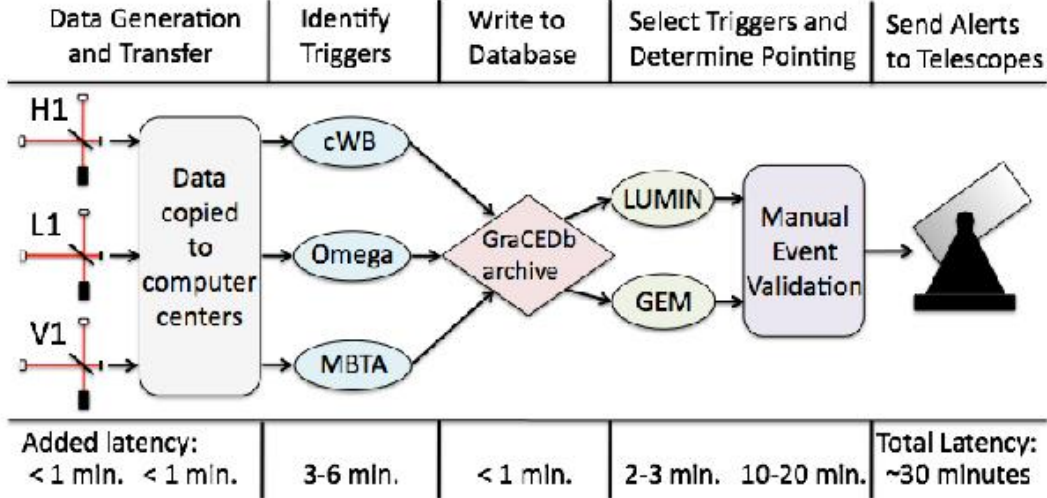


Figure 8: The low latency pipeline used to generate GW triggers into sky tiles for a telescope. The telescope eventually receives a tile with location and time information and points to the correct position in the sky.[13]

4 GW Data Generation

The data that the simulation analyzes is in the form of sky tiles. A single sky tile has characteristics of location, in RA dec celestial coordinates, and an associated GPS time. These tiles are generated through a pipelined process that begins with GW detections taken by the interferometers. These detections are then processed in a few key steps resulting in the sky tiles. It is key for this pipeline to have a relatively low latency because the telescopes need to respond as soon as possible after a GW detection. The current latency is approximately 30 minutes from detector to telescope.

4.1 Skymap Algorithm

The first step in the pipeline is to generate a sky map. For each GW trigger, a corresponding sky map is generated that covers a

portion of the sky in the vicinity of the trigger. This approximate location is obtained from the data received from the detectors. Each pixel in the sky map is assigned a probability of the GW source being located there. As stated earlier, the location of GW sources are not very precise which is why probabilities must be used. The result is the "original skymap" in Figures 9 and 10.

4.2 Weighted Skymap

The original skymap is generated using only the GW data obtained from the detectors. For more accurate results the pipeline creates what is called a weighted sky map. After the first sky map is generated, this function compares each pixel to a galaxy catalogue. This catalogue contains all known galaxies out to 50 mega parsecs. Each pixel is checked to see if there is a galaxy in it's immediate region. If a galaxy is found, a

higher or lower probability is calculated for the pixel based on the mass of the galaxy and the distance of the galaxy from earth. If no galaxy is found the probability is set to zero because a GW source cannot exist if there is nothing but empty space. The result is the "weighted skymap" in Figures 9 and 10. Because the universe is mostly empty space, it is important to perform this comparison in order to rule out locations that a GW source could not possibly reside.

4.3 Sky Tiling

When the weighted sky map is complete, the pipeline generates sky tiles. The tiles are produced using the data in the weighted sky map and the field of view of the telescope. Each tile has an area that match the FOV. Each tile is generated by finding an area on the sky map equal to the FOV that has the highest overall probability when combining all of the pixels enclosed by that area. The location of the center of the tile is taken from the sky map and assigned as the RA and dec coordinates of the tile. These coordinates can be read and the telescope can search this portion of the sky for an electromagnetic signal. Some telescopes have the capability of taking multiple observations as it scans across a region of the sky. This is called a mosaic. When a telescope can do this, the sky tiling algorithm generates multiple tiles with the highest probability values. This is done by finding the most probable tile, then disregarding the pixels enclosed by the first tile and computing the next most probable tile with the remaining pixels. The process is repeated for the number specified in the "mosaic" variable of the telescope. Mosaic = 5 generates five tiles per event.

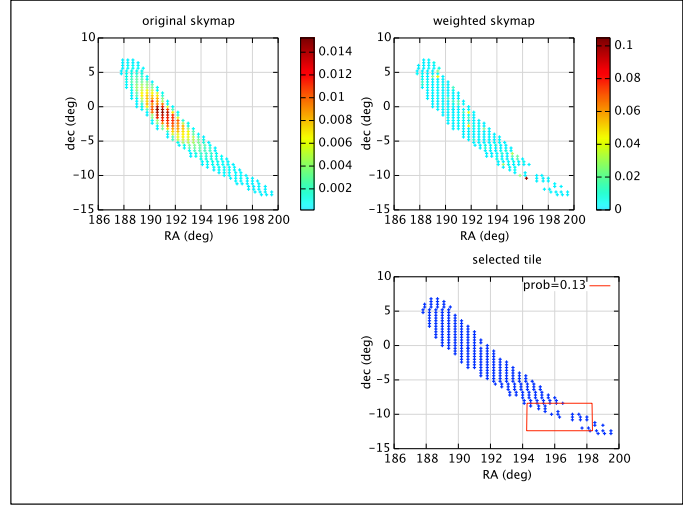


Figure 9: Original and weighted sky map with the corresponding most probable sky tile. The tile has the same dimensions as the field of view of the telescope being used.

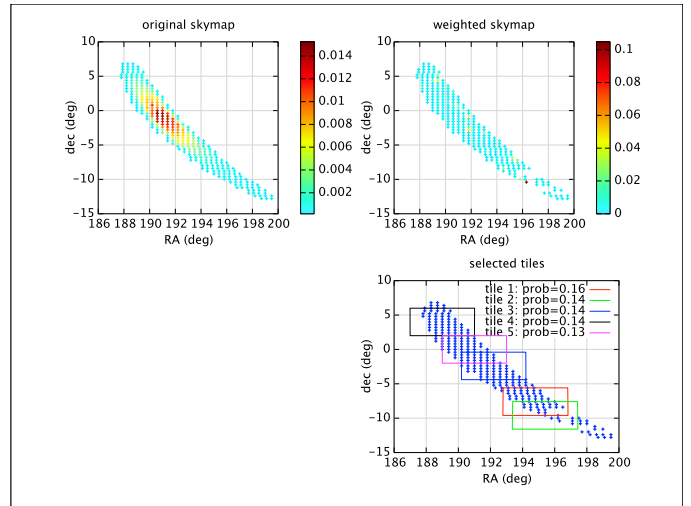


Figure 10: Original and weighted sky maps with the corresponding five most probable sky tiles. When each tile is made, the pixels enclosed by the previous tile are disregarded and the next most probable region is calculated.

Table 1: Telescope Characteristics

Name	Latitude	Longitude	Height	Width	Mosaic	Aperture	Exposure
Zadko	-31.35666	-115.71361	0.38	0.38	5	1	60
ROTSE A	-31.27336	-149.06119	1.85	1.85	1	.25	60
ROTSE B	23.27166	-16.5000	1.85	1.85	1	.25	60
ROTSE C	36.82500	-30.3333	1.85	1.85	1	.25	60
ROTSE D	30.67158	104.02225	1.85	1.85	1	.25	60
TAROT N	43.752222	-6.923889	1.86	1.86	1	.25	180
TAROT S	-29.26083	70.73222	1.86	1.86	1	.25	180
Skymapper	-31.27333	149.06444	2.37	2.4	1	1	60
PTF	33.35583	116.86388	3.5	2.3	1	1	60
QUEST	33.35583	116.86388	3.6	4.6	1	1	60
Pi of The Sky	-22.95333	68.18000	20	20	1	0.1	10

5 The Simulation

The approximate location in the sky of the gravitational wave source is now represented by the sky tile or tiles. The event also has a GPS time and a scale associated with it’s identity. The GPS time is the time of the detection and the scale is the strength of the GW source. The other object used in the simulation is the telescope. A telescope in the code is a structure containing the variables "name", "latitude", "longitude", "width", "height", "mosaic", "aperture", and "exposure". The information for the 10 telescopes used for the simulations can be found in Table 1. These variables completely describe the telescope that is to be analyzed by the simulation. The simulation uses the variables associated with the gravitational wave trigger and the telescope to explore five key factors that contribute to the ability or inability to complete an observation.

5.1 Observable Function

The "observable" function computes whether or not the gravitational wave source is in the observable sky of the telescope. The location of the sky tile is given in celestial coordinates, which is a global coordinate system (celestial coordinates do not change from place to place on earth, they remain constant). Thus it is impossible to tell whether or not the source is in the visible sky by simply looking at these coordinates. The function determines this critical information by transforming the RA dec coordinates of the source to the local altitude of the source. The local altitude of an object in the sky is it’s angle relative to the horizon (positive above, negative below) from a specific observation point on the surface of the earth. This transformation is completed using equation 1.

$$\sin h = \sin \phi \cdot \sin \delta + \cos \phi \cdot \cos \delta \cos H \tag{1}$$

In Equation 1, h is the local altitude above the horizon, ϕ is the latitude of the telescope, positive if in the northern hemisphere negative in the southern, and δ is the declination coordinate of the sky tile. H is called the local hour angle measured westward from the south. It is computed using Equation 2.

$$H = \theta - L - \alpha \quad (2)$$

In Equation 2, θ is the sidereal time at Greenwich England, L is the observers longitude (positive west, negative east from Greenwich), and α is the right ascension of the sky tile. Finally, Equation 1 can be solved for h by taking the arc sine of both sides.

$$h = \arcsin[\sin \phi \cdot \sin \delta + \cos \phi \cdot \cos \delta \cos H] \quad (3)$$

Here, h is the relative angle between the tile location and the horizon of the observer. If this value is positive, the tile is in the observable sky. If it is negative, the tile is below the horizon line and not in the observable sky. The function checks the value of h and simply returns a "1" if the value is positive (observation is possible) or a "0" if the value is negative (observation is impossible). The function is declared in the code using Equation 4.

$$\text{Observable}(GPS, long, lat, RA, DEC) \quad (4)$$

GPS is the GPS time of the event, $long$ is the longitude of the telescope, lat is the latitude

of the telescope, RA is the right ascension of the sky tile, and DEC is the declination of the sky tile.

5.2 Sun Function

The "sun" function computes the position of the sun in the sky at the observers location to determine whether or not it is dark enough to make an optical observation. `Sun()` calls a separate function called "solarElevationAngle" which directly calculates the angle of the sun relative to the local horizon at the given time.

5.2.1 Solar Coordinates

Calculating the precise coordinates of the Sun requires the consideration of many parameters as well as the use of lengthy equations. However, for the purposes of this simulation a simplified algorithm that is accurate to 0.01 degrees is sufficient. The motion of the earth is assumed to be purely elliptical, neglecting perturbations by the Moon and planets.

The first step is to calculate the time T by means of Equation 5.

$$T = \frac{JD - 2451545.0}{36525} \quad (5)$$

This quantity needs to be extremely precise and calculated with a high number of decimal places. T is expressed in centuries, so an error of 0.00001 in T corresponds to an error of 0.37 days in time. The value of T is

then used to calculate several other important quantities. The geometric mean longitude of the sun is given by Equation 6.

$$L_0 = 280.46646 + 36000.76983 \cdot T + 0.0003032 \cdot T^2 \quad (6)$$

The mean anomaly of the sun is given by Equation 7.

$$M = 357.52911 + 35999.05029 \cdot T - 0.0001537 \cdot T^2 \quad (7)$$

The eccentricity of earth's orbit is given by Equation 8.

$$e = 0.016708634 - 0.000042037 \cdot T - 0.0000001267 \cdot T^2 \quad (8)$$

The sun's equation of the center is given by Equation 9.

$$C = (1.914602 - 0.004817 \cdot T - 0.000014 \cdot T^2) \cdot \sin M + (0.019993 - 0.000101 \cdot T) \sin(2M) + 0.000289 \cdot \sin(3M) \quad (9)$$

From these values the sun's true longitude is determined by using Equation 10.

$$\odot = L_0 + C \quad (10)$$

From here the Sun's right ascension α and declination δ can be expressed using Equations 13 and 14 where ϵ is the obliquity of the ecliptic.

$$\epsilon = 23.439999 \quad (11)$$

$$\tan \alpha = \frac{\cos \epsilon \cdot \sin \odot}{\cos \odot} \quad (12)$$

$$\sin \delta = \sin \epsilon \cdot \sin \odot \quad (13)$$

Once the RA and dec coordinates of the Sun are known they are transformed into local coordinates by means of Equations 1, 2 and 3.[10] The "solarElevationAngle" function then returns a value that is the angle between the location of the Sun and the observers local horizon. The accuracy of this function was tested using data from the United States Naval Observatory. The simulation is accurate to within a tenth of a degree. The direct comparisons can be seen in Table 2.

5.2.2 Analysis of Sun's Altitude

Once the "solarElevationAngle" function is called, the "sun" function now has the value of the Sun's local altitude as viewed by the telescope at a specific location on earth. In the case of determining day or night, it is not simply a matter of whether this angle is positive or negative. It may still be too bright for a telescope to make an observation even if the Sun is below the horizon.

Table 2: Sun’s Altitude from ”Sun” Function and USNO Data.[16]

Source ↓ Time ⇒	14:00	14:10	14:20	14:30	14:40	14:50	15:00
”Sun” Function	68.027	67.500	66.801	65.945	64.948	63.827	62.599
”USNO Data”	68.0	67.5	66.8	65.9	65.0	63.8	62.6

The ”sun” function compares the local altitude of the Sun to the values given in Table 3. Astronomical twilight is defined to be dark enough for any astronomical observation to be made.[15] Thus when the ”sun” function checks the value of the Sun’s altitude, anything greater than -12° results in a ”0” being returned by the function and anything less than -12° results in a ”1” being returned by the function.

Table 3: Definitions of Sun’s Altitude[15]

Classification	Altitude of Sun
Day	$\theta \geq 0^\circ$
Civil Twilight	$-6^\circ \leq \theta < 0^\circ$
Nautical Twilight	$-12^\circ \leq \theta < -6^\circ$
Astronomical Twilight	$-18^\circ \leq \theta < -12^\circ$
Night	$\theta < -18^\circ$

The ”1” and the ”0” once again correspond to a possible or impossible observation, respectively. The ”sun” function is declared in the code using Equation 14.

$$Sun(GPS, long, lat)$$

(14)

Here GPS is the GPS time of the gravitational wave event, long is the longitude of the telescope and lat is the latitude of the telescope.

5.3 Moon Function

The ”moon” function determines two important pieces of information about the Moon; it’s location and it’s illumination. Using this data the function can see if the Moon is blocking the tile and whether it’s brightness has any effect on a possible observation. This information is combined to make a final decision on whether or not the Moon allows or prevents an optical observation.

5.3.1 Lunar Coordinates

The process for calculating the position of the Moon is similar to that of calculating the position of the Sun. There are several values that must be computed and then combined together to obtain the coordinates. In order to obtain a precise value for the position of the Moon it is necessary to take into account hundreds of periodic terms in the Moon’s longitude. However, the accuracy that is necessary for this simulation requires the use of only the most important of these terms. The process starts by getting

the value of T from Equation 5. The same goes here as in the solar coordinate calculation that a high number of decimal places is included. Next, the Moon's mean longitude is defined by Equation 15.

$$L' = 218.3164477 + 481267.88123421 \cdot T - 0.0015786 \cdot T^2 + \frac{T^3}{538841} - \frac{T^4}{65194000} \quad (15)$$

The mean elongation of the Moon is defined by Equation 16.

$$D = 297.8501921 + 445267.1114034 \cdot T - 0.0018819 \cdot T^2 + \frac{T^3}{545868} - \frac{T^4}{113065000} \quad (16)$$

The Sun's mean anomaly is defined by Equation 17.

$$M = 357.5291092 + 35999.0502909 \cdot T - 0.0001536 \cdot T^2 + \frac{T^3}{24490000} \quad (17)$$

The Moon's mean anomaly is define by Equation 18.

$$M' = 134.9633964 + 477198.8675055 \cdot T + 0.0087414 \cdot T^2 + \frac{T^3}{69699} - \frac{T^4}{14712000} \quad (18)$$

The Moon's argument of latitude (the mean distance of the Moon from its ascending node) is defined by Equation 19

$$F = 93.2720950 + 483202.0175233 \cdot T - 0.0036539 \cdot T^2 - \frac{T^3}{3526000} + \frac{T^4}{863310000} \quad (19)$$

Finally there are three further arguments that are needed to complete the computation. These arguments are defined in Equation 20.

$$\begin{aligned} A_1 &= 119.75 + 131.849 \cdot T \\ A_2 &= 53.09 + 479264.290 \cdot T \\ A_3 &= 313.45 + 481266.484 \cdot T \end{aligned} \quad (20)$$

Of the hundreds of periodic terms, the simulation uses the ten most important terms to achieve a necessary level of accuracy. There are two sums that are calculated, $\sum l$ and $\sum b$. The complete sums are defined in Equations 21 and 22.

$$\begin{aligned} \sum l &= 62887744 \cdot \sin M' + 1274027 \cdot \sin(2D - M') \\ &+ 658314 \cdot \sin 2D + 213618 \cdot \sin 2M' \\ &- 185116 \cdot \sin M - 114332 \cdot \sin 2F \\ &+ 58793 \cdot \sin(2D - 2M') + 57066 \cdot \sin(2D - M - M') \\ &+ 53322 \cdot \sin(2D + M') + 45758 \cdot \sin(2D - M) \end{aligned} \quad (21)$$

$$\begin{aligned} \sum b &= 5128122 \cdot \sin F + 280602 \cdot \sin(M' + F) \\ &+ 277693 \cdot \sin(M' - F) + 173237 \cdot \sin(2D - F) \\ &+ 55413 \cdot \sin(2D - M' + F) + 46271 \cdot \sin(2D - M' - F) \\ &+ 32573 \cdot \sin(2D + F) + 17189 \cdot \sin(2M' + F) \\ &+ 9266 \cdot \sin(2D + M' - F) + 8822 \cdot \sin(2M' - F) \end{aligned} \quad (22)$$

Any periodic term that contains the angle M depends on the eccentricity of the Earth's orbit around the Sun. To take this into account any term with M or $-M$ is multiplied by the value E and any term containing $2M$ or $-2M$ is multiplied by E^2 . E is defined by Equation 23.

$$E = 1 - 0.002516 \cdot T - 0.0000074 \cdot T^2 \quad (23)$$

Finally, an additive term is included in both sums. The terms including A_1 are due to the action of Venus, the terms involving A_2 is due to Jupiter, and the terms with L' are due to the flattening of the earth. The additive term for $\sum l$ is defined by Equation 24 and the additive term for $\sum b$ is defined by Equation 25.

$$\begin{aligned} \sum l_{Add} = & 3958 \cdot \sin A_1 + 1962 \cdot \sin(L' - F) \\ & + 318 \cdot \sin A_2 \end{aligned} \quad (24)$$

$$\begin{aligned} \sum b_{Add} = & -2235 \cdot \sin L' + 382 \cdot \sin A_3 \\ & + 175 \cdot \sin(A_1 - F) + 175 \cdot \sin(A_1 + F) \\ & + 127 \cdot \sin(L' - M') - 115 \cdot \sin(L' + M') \end{aligned} \quad (25)$$

Once this is completed the geocentric coordinates of the Moon are computed. The ecliptic longitude is given by Equation 26 and the ecliptic latitude is given by Equation 27.

$$\lambda = L' + \frac{\sum l}{1000000} \quad (26)$$

$$\beta = \frac{\sum b}{1000000} \quad (27)$$

In order to use the location of the Moon to compute the angular distance between the Moon and the sky tiles, the coordinates are converted from geocentric to celestial coordinates by means of Equation 28 and 29. The right ascension α of the Moon is defined by Equations 28 and the declination δ of the Moon is defined by Equation 29.[10]

$$\tan \alpha = \frac{\sin \lambda \cdot \cos \epsilon - \tan \beta \cdot \sin \epsilon}{\cos \lambda} \quad (28)$$

$$\sin \delta = \sin \beta \cdot \cos \epsilon + \cos \beta \cdot \sin \epsilon \cdot \sin \lambda \quad (29)$$

5.3.2 Moon Illumination

The brightness of the Moon can have a large effect on the observability of an object in the night sky. Rather than go through the rigor of finding a mathematical solution to the phase of the moon at a given time, the simulation uses a table of data provided by the United States Naval Observatory (USNO). The table provides a percentage that represents the fraction of the Moon's disk that is illuminated for any given day. Each table contains one years worth of Moon illumination data. To obtain a value for the Moon illumination the simulation simply extracts the data from the correct table corresponding to the day of the year that the GW event occurred.

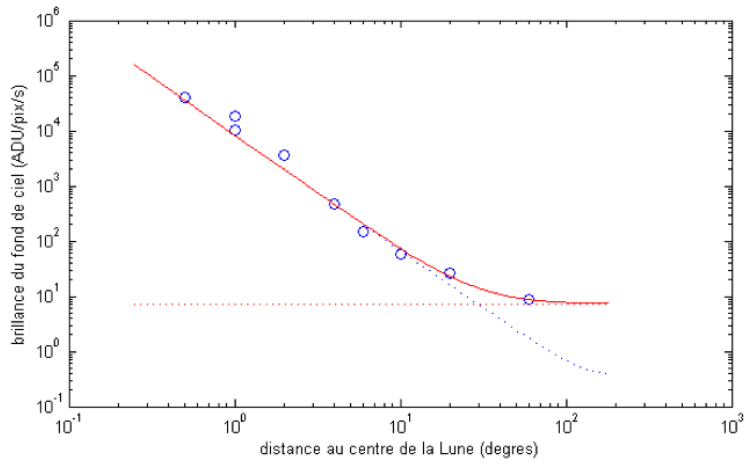


Figure 11: The brightness of the sky based on the distance from the center of a full moon. The red horizontal line represents the background brightness if the moon was not present. The intersection of the red and blue lines represents the minimum distance from the full moon that an object must be to observe it.

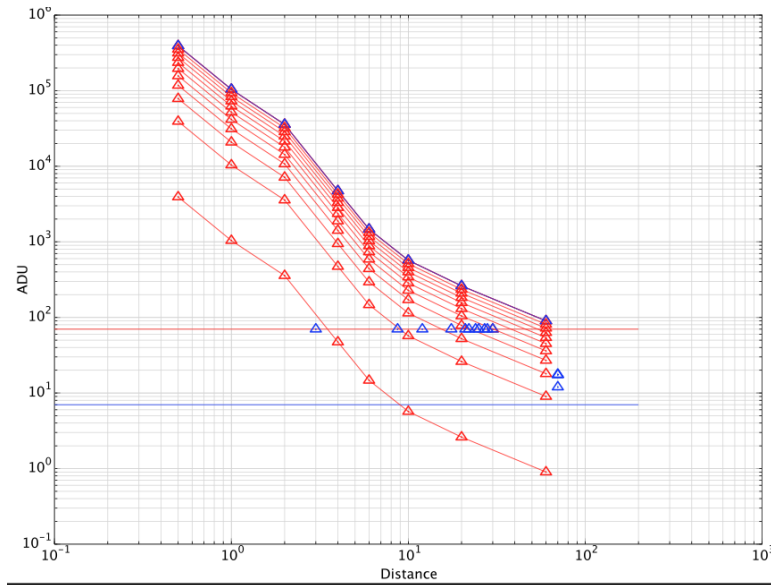


Figure 12: Brightness of sky vs distance from moon plotted for each illumination percentage, with the top curve representing 100 percent illumination and the bottom 1 percent illumination. The intersection points with the background brightness are marked in blue.

5.3.3 Determining the Minimum Distance

Once the celestial coordinates and the illumination of the Moon are known the simulation is able to compute the minimum distance that the GW source can be from the moon without interrupting an observation. There is no way to directly compute this distance (at least that we know of), so data from previous observations is used. The graph in Figure 11 shows observations taken by TAROT South. It plots the brilliance of a point in the sky against the distance the point is from the center of a full moon. The red horizontal line represents the brilliance of the night sky if no Moon were present. The intersection point of the red and blue lines shows the minimum angular distance that an observation must be taken in order to have no interference from the Moon's brightness.

Because the moon goes through phases, additional data for every possible moon phase was extracted from this graph. The full moon represents a 100 percent illumination, so for each data point a ratio was constructed in the form of Equation 30.

$$\frac{100}{CurrentBrilliance} = \frac{NewPercentage}{NewBrilliance} \quad (30)$$

This was then solved for *NewBrilliance* and the new data point plotted on the original graph. This was done for each data point to obtain a new curve for the specified percentage. A curve was plotted for each percentage value from 100 to 0 in increments of 10. The curves for each illumination percentage are

plotted in Figure 12, with the blue markers indicating the intersection between the curve and the background brightness of the sky. These points mark the minimum distance from the moon for each illumination percentage.

The final step in retrieving all of the necessary data was to make a plot of moon illumination vs minimum distance by using the information generated in Figure 13. This plot, shown in Figure 14, provides the simulation with a minimum distance for any moon illumination value between 0 and 100.

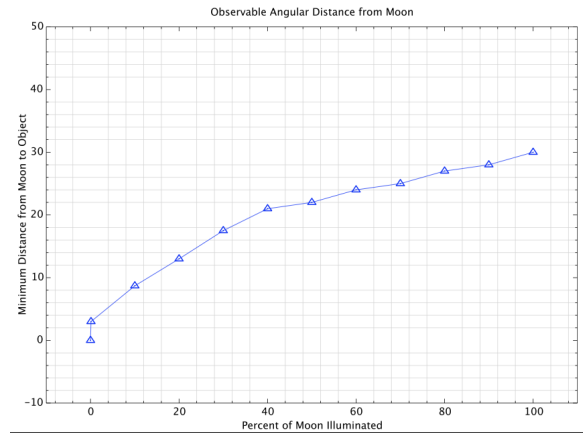


Figure 13: Plot of percentage of Moon illuminated vs minimum distance. This plot provides the minimum distance the sky tile must be from the moon given the Moon's illumination percentage.

5.3.4 Final Moon Analysis

Once the position of the moon is known, the angular distance between the moon and the sky tile is computed. The angular distance in degrees between two celestial points is defined by Equation 31.[10]

$$\begin{aligned} \cos D &= \sin dec_1 \cdot \sin dec_2 \\ &+ \cos dec_1 \cdot \cos dec_2 \cdot \cos(RA_1 - RA_2) \end{aligned} \quad (31)$$

This equation is applied using the RA and dec of the Moon as computed earlier and the RA and dec of the sky tile which is generated in the sky tiling algorithm. The illumination percentage of the moon is then found using the "moonIllumination" function and the minimum distance from the Moon corresponding to this percentage is taken from the data generated from the plot in Figure 13. All of this is done within the "moon" function and is called in the code using the command in Equation 32.

$$Moon(GPS, RA_{tile}, DEC_{tile}) \quad (32)$$

In Equation 32, GPS is the GPS time and RA_{tile} and DEC_{tile} are the coordinates of the sky tile. The angular distance between the sky tile and the Moon is then compared to the minimum distance. If the distance is less than the minimum distance, then the observation is occurring too close to the Moon and the sky is too bright. If the distance is greater than the minimum distance then the Moon has no effect on an observation of that part of the sky. The "moon" function returns a "1" if the observation is possible and a "0" if it is not.

5.4 Weather Function

Weather is a very important variable when it comes to observing the night sky. The "weather" function use data from the Food and Agriculture Organization of the United

Nations (FAO) to determine whether or not the sky is clear enough to observe the sky tiles. Once a value is obtained for the weather, a random number generator is used to simulate the probabilistic nature of weather conditions.

5.4.1 Weather Data

FAO uses gridded data maps to generate images such as the one found in Figure 14. The raw data for this image is in the form of a giant matrix that spans the entire surface of the earth. Each $.5^\circ \times .5^\circ$ area on earth's surface is assigned a value that represents the percentage of time when bright sunshine is recorded during the day. This is directly linked to cloudiness, with full cloud cover being equal to 0 percent of sunshine fraction.^[9] These values are averages that have been obtained over years of data analysis.

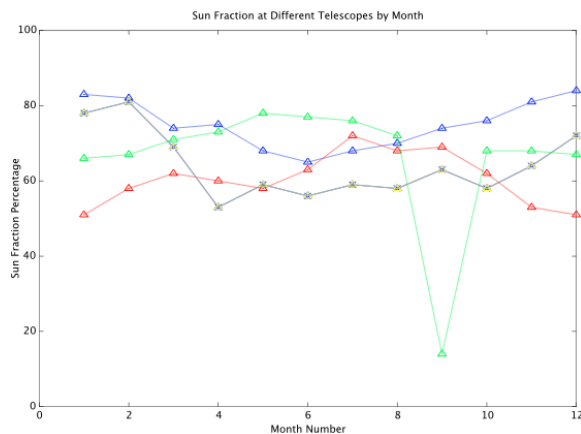


Figure 15: Sun fraction by month at the locations of Zadko (blue), TAROT North (red), Pi of the Sky (green) and TAROT South (grey). As expected, the summer months of each telescope have higher sun fractions and the winter months have lower sun fractions.

The simulation utilizes 12 separate

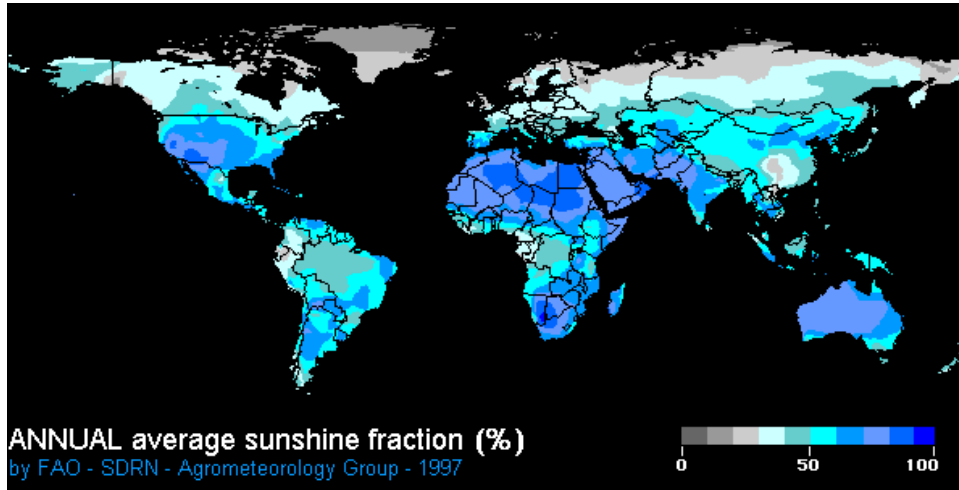


Figure 14: World map of annual average sunshine fraction provided by FAO. The raw data used to generate this map is a giant grid spanning all points on the surface of the earth. This raw data is available on the FAO website and is used in the "weather" function of the simulation. [9]

weather grids, one for each month. The simulation retrieves data from the matrix by matching the latitude and longitude of the telescope to the proper matrix element on the data map. The sun fraction value can then be used to determine the weather. A plot of the sun fraction at Zadko, TAROT N, Pi of the Sky, and TAROT S is provided in Figure 15.

5.4.2 Determining the Weather

Once the function obtains a sun fraction percentage from the weather map, it uses this and a random number generator to simulate the current weather. A random number is generated between 0 and 100. If the number is less than or equal to the sun fraction percentage, then the sky is determined to be clear. If the number is greater than the sun fraction percentage, the sky is determined to be cloudy. The value taken from the weather map represents the "chance" of the weather

being clear. Using the random number generator and comparing the number to the percentage using this method properly simulates the randomness seen in weather on a day to day basis. The "weather" function is called in the code using the command in Equation 33.

$$Weather(GPS, long, lat) \tag{33}$$

In Equation 33 GPS is the GPS time, long is the longitude of the telescope, and lat is the latitude of the telescope. This function returns a "1" if the sky is determined to be clear and a "0" if the sky is determined to be cloudy.

5.5 Tile Check Function

As stated earlier, it is extremely difficult to perform electromagnetic follow-ups of gravitational wave triggers because they are

tough to precisely locate in the sky. The coordinates of the tiles that are used to generate the directions for the telescopes to point are not always accurate. The ability of the sky tiling algorithm to generate accurate tiles is directly related to the scale of the gravitational wave event. The higher the scale, the better the locating ability of the tiling algorithm. A percentage of the tiles sent to the telescope will not contain the actual GW event within it's area. This must be taken into account when calculating the probability that a telescope will be able to perform a follow-up observation. For each tile, the simulation checks to see if the coordinates of the GW injection are within the field of view of the tile.

The coordinates of each tile correspond to a point in the very center of the tile. Although each tile takes the shape of a rectangle or square, the tile check function approximates it as a circle to keep the algorithm simple. The radius of the circle is taken to be the width of the tile divided by two. The angular distance between the center of the tile and the GW source is calculated by again using Equation 31. If this distance is less than the radius of the circle, the event is within the tile and an observation can be made. If this distance is greater than the radius of the circle then the event is outside tile and an observation cannot be made. Figure 32 shows a plot of the percentage of tiles that are accurate vs scale of the GW source. It would be advantageous to generate more accurate tiles, and this issue will be addressed in future work. Even for higher scales, only about 30 percent of the tiles accurately locate the GW source. The function is called within the simulation code using the com-

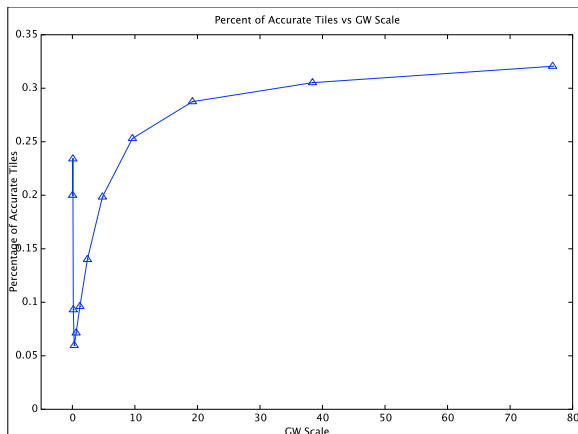


Figure 16: Plot depicting the accuracy of the sky tiling algorithm based on the scale of the GW source. Even with high scales, only about 30 percent of the tiles contain the GW source.

mand in Equation 34.

$$\begin{aligned}
 & \text{withinTile}(RA_{inj}, DEC_{inj}, RA_{tile}, \\
 & \quad DEC_{tile}, width)
 \end{aligned}
 \tag{34}$$

In Equation 34 RA_{inj} is the right ascension of the GW event, DEC_{inj} is the declination of the GW event, RA_{tile} is the right ascension of the sky tile, DEC_{tile} is the declination of the sky tile, and $width$ is the width of the field of view of the telescope. The function returns a "1" if the GW source is within the area of the tile and returns a "0" if the source is outside the area of the tile.

5.6 Limiting Magnitude Function

The brightness or observability of an object in the sky is quantified by it's magnitude. A higher magnitude corresponds to a brighter,

more observable object and a lower magnitude corresponds a dimmer object that is harder to observe. There is a point where an object can be so dim that it is not observable by a telescope. The value is different for every telescope and is directly related to it's exposure time and diameter. This threshold is called the limiting magnitude. The limiting magnitude of a telescope is defined by Equation 35.

$$M_{limiting} = 18.2 + 2.5 \cdot \log\left(\frac{exp}{30}\right) + \frac{\log\left(\frac{d}{.25}\right)}{\log(1.59)} \quad (35)$$

In Equation 35 Exp is the exposure time in seconds of the telescope, d is the diameter of the telescope, and log is base 10.

The longer the exposure time, the lower the limiting magnitude of the telescope. A longer exposure time allows for more light to be absorbed by the imaging process thus resulting in dimmer objects being seen. However, longer exposures may result in unwanted light being imaged as well. This is why it is critical that telescopes be located in secluded areas that are far from external influences such as "light pollution" from large cities. The effect of varying exposure times is given in Figure 17.

Once the limiting magnitude is found, it is compared to the magnitude of the GW source (which is also computed directly by the function). If the source magnitude is less than the limiting magnitude of the telescope, then an observation is not possible. If the source magnitude is greater than the limiting magnitude, then an observation can be made. The function returns a "1" for a possible observation or a "0" if an observation is not possible. The "limitingMagni-



Figure 17: Longer exposure (left) vs shorter exposure (right) of the same celestial objects. A longer exposure allows consistent sources of light in the sky to be imaged more clearly.[4]

tude" function is called in the code using the command in Equation 36.

$$LimitMag(time, distance, diameter, exp) \quad (36)$$

In Equation 36 Time is the amount of time in seconds after the gravitational wave event, distance is the distance from the earth to the source, diameter is the diameter of the telescope, and exp is the exposure time in seconds of the telescope.

Due to the low latency of the pipeline that transfers data from the gravitational wave detectors to the telescope for pointing, any astrophysical event that is strong enough to create gravitational waves that are detectable on earth will be bright enough to observe in the night sky. The simulations that are presented in this paper are assuming that an observation is attempted immediately after a telescope receives a trigger from the GW detectors. Therefore, the limiting

magnitude is not a factor that is considered. However, this becomes important when trying to observe an event hours or days after it occurs. Large events have "afterglows" that are often observable for an extended period of time after an initial electromagnetic detection, but the magnitude decays with time. An example GRB afterglow light curve is provided in Figure 18. In this case it will

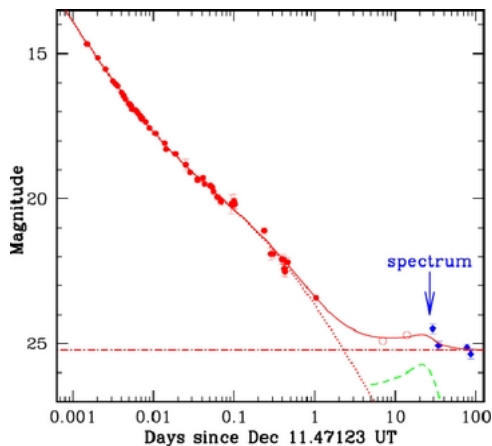


Figure 18: This plot shows how the magnitude of GRB 021211 decays with time.

be important to know the time dependent magnitude of the GW event to determine if an observation can be performed. A prime example of when this will be used is when a telescope cannot view an object because it is day at the time it receives an alert. However, if the telescope attempts to make an observation once it becomes dark (lets say 12 hours later), will the GW source still have a large enough magnitude to be seen? Future simulations using the "limitingMagnitude" function will be able to answer this question. The ability of telescopes to make observations over larger windows of time will likely increase the probability of performing a successful electromagnetic follow-up of a

gravitational wave detection.

5.7 Total Simulation

Each of the functions discussed in the previous sections make up a piece of a single overall simulation. In the final program, each function is called and returns a "1" corresponding to the event being observable or a "0" corresponding to the event not being observable. Close to 100,000 "fake" gravitational wave events having various times, locations, and scales are injected into the pipeline and each tile is then analyzed by each function. If a tile receives a "0" from any of the 6 functions, the event is deemed unobservable. If a tile receives a "1" from all 6 functions then the event is deemed observable.

Finally, after all events are analyzed they are separated by GW scale and a plot of scale vs probability of observation is generated. The simulation that completely analyzes a single tile is called using the command in Equation 37.

$$\text{OpticalSimulation}(GPS, RA_{inj}, DEC_{inj}, RA_{tile}, DEC_{tile}, long, lat, aper, exp, width) \quad (37)$$

In Equation 37, GPS is the GPS time, RA_{inj} is the right ascension of the GW source, DEC_{inj} is the declination of the GW source, RA_{tile} is the right ascension of the sky tile, DEC_{tile} is the declination of the sky tile, $long$ is the longitude of the telescope, lat is the latitude of the telescope, $aper$ is the aperture of the telescope, exp is the exposure of the telescope, and $width$ is the width of the telescope's field of view. This function

is then placed in a for-loop that analyzes every tile from every "fake" GW injection in the data set. The final call to produce the plot of scale vs probability of observation in Octave is given by Equation 38.

$$TotalSim() \tag{38}$$

*Note: GPS time is the only format of time that is injected into the pipeline. However, some functions need the time of the event in other formats such as year, month, day of year, sidereal time, Greenwich local time, Julian Ephemeris Day (JDE), or UTC time. Each function converts the given GPS time to the value it needs on it's own using *tconvert()* in the LALApps software package. LALApps can be downloaded for free from the LIGO Data Analysis Software Working Group.[3]

Also, the sign convention for the longitude and latitude values of the telescope location are positive north, negative south and positive west, negative east. This is different from the standard convention of positive north, negative south and negative west, positive east. For example, google maps uses the latter (+N, -S, +E, -W) when searching by coordinate locations.

6 Results

The first run of simulations was done on a single telescope. TAROT South was chosen because of it's location's well documented weather data and it's similarity in field of view to other telescopes that are prime candidates for this program. Figure 19 shows

the GW scale vs probability of observation plot for a full simulation of all GW events in the database. A maximum probability of about 6 percent for the highest GW scale may seem discouragingly low. However, looking back on Figure 16 shows that the tiling algorithm alone only has a probability of observation of about 30 percent. Add in five more factors that determine observability and it makes sense to see such low values. Although the probabilities may be lower than expected, the overall shape of the plot fits what is predicted. Besides a small jump at one of the lower scales, the probability increases as GW scale increases.

An advantage to the way the simulation is coded is the ability to change many parameters quite easily. This allows for many different types of simulations to be run without having to overhaul large blocks of code. An example of this is to assume that a telescope is not available for use during daylight hours. This can be simulated by disregarding the "sun" function and only plotting GW events that occur during dark hours. A plot of the observation probability of "all night" GW events at TAROT South is provided in Figure 19. As expected the probability at each point increases because the sun function is no longer a limiting factor in the simulation. However, the results also deviate from what is expected in the shape of the graph. The lowest GW scale events have a probability almost equal to that of the highest GW scale events. This is certainly a feature that will be examined in future tests in order to either understand the unpredicted behavior or fix a problem in the code.

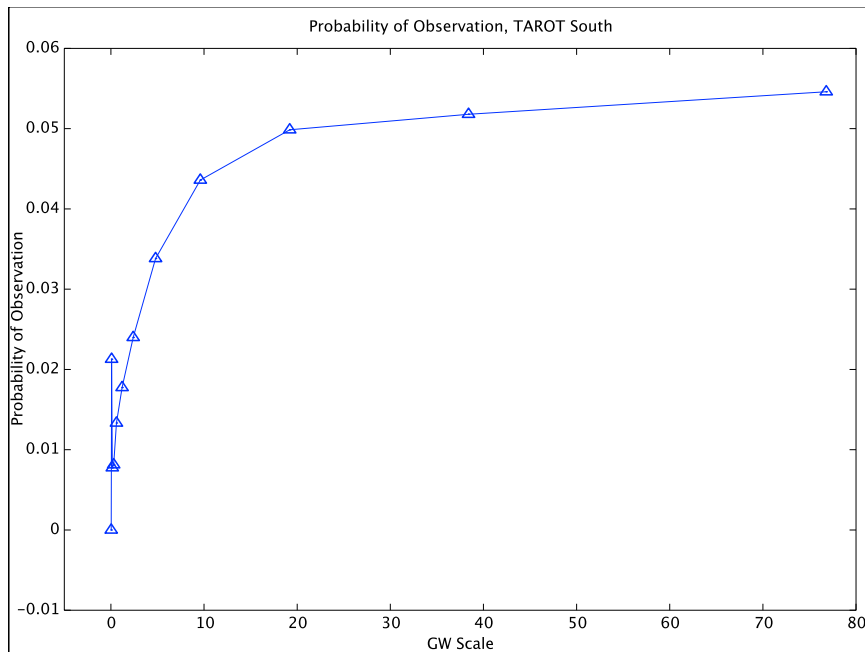


Figure 19: Full simulation of observation probability vs GW scale for TAROT South. The plot behaves as expected, the probability increases with increasing scale.

7 Conclusions

The objective of this paper is to provide a detailed description of how the simulation works and to explain why it is structured the way that it is. The plots provided are meant to demonstrate the capabilities of the simulation and are by no means to be taken as final results. These few plots are only the very start of a project that has vast scientific capabilities. When more simulations are completed and necessary corrections and improvements are made, this project will be able to provide answers to many unknown questions regarding electromagnetic follow-up observations. Even so, these plots provide further testimony to the fact that gravitational wave sources are extremely difficult to locate, making it a daunting task to per-

form an electromagnetic follow-up observation. It also shows that the simulations may not be totally accurate quite yet.

However, even these preliminary results provide valuable information. It is clear that the tiling algorithm has much room for improvement seeing that only about 30 percent of the generated tiles are accurate to within the field of view of a telescope. This may be due to the fact that the algorithm is not good enough and must be changed. It may also be that gravitational wave sources are inherently difficult to locate and the algorithm is already as accurate as it possibly can be. It is also quite obvious that a single telescope will not suffice for an electromagnetic follow-up program. A global network of telescopes providing a maximum amount of sky coverage will certainly be needed to

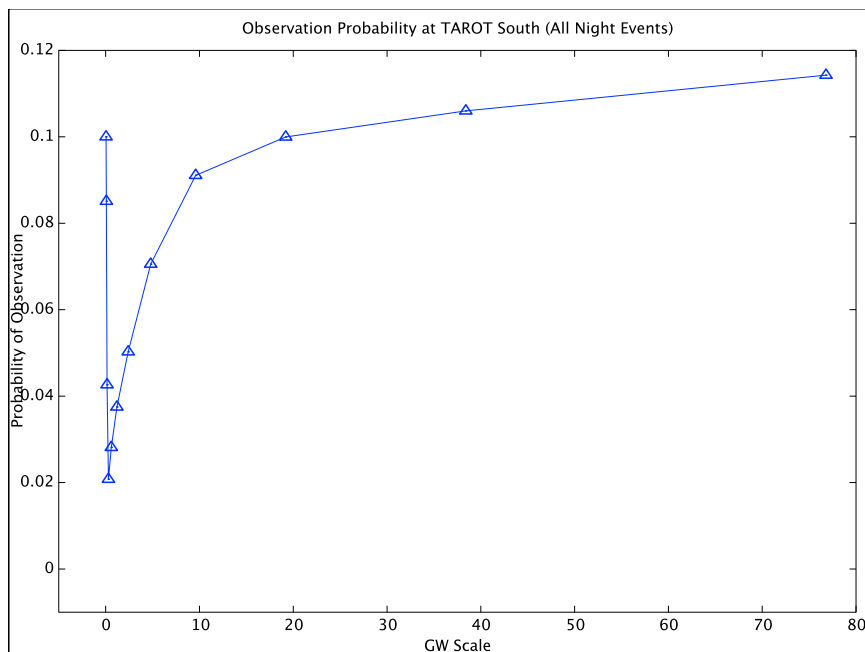


Figure 20: Observation Probability at TAROT South assuming all event triggers are received during the night.

raise the observation probability to the preferred level.

8 Future Work

There are many scientific paths that can be taken from this point in the project. Many plans are already in mind as to what steps will be taken next. A few preliminary ideas are outlined in the following sections.

8.1 Small Fixes

The question as to why unexpected deviations from the predicted results are being seen in the simulation needs to be addressed. More simulations will be run with the hopes of either finding pieces to fix within the code or explaining why the nature of the

simulation is different from what was expected. There is experimental data from the first electromagnetic follow-up program that can be used to compare with the simulation results, providing a general idea of what should be found.

8.2 Improvement of Tiling Algorithm

Only about 30 percent of the tiles from the current tiling algorithm contain the actual gravitational wave event coordinates. This is the main cause of the extremely low overall probabilities seen in Figure 18. The algorithm will be tested and reviewed to determine where changes can be made. More accurate tiles alone will allow telescopes to search the sky in the proper locations, re-

sulting in a drastic increase in the probability of a follow-up observation.

8.3 More Telescopes

The simulation has only been run for one telescope, TAROT South. Individual simulations for all of the telescopes outlined in Table 1 as well as others will be completed. Comparing and contrasting the observation probability vs GW scale graphs from different telescopes will allow us to determine which locations on earth and what telescope characteristics provide the greatest chances of an observation.

8.4 Global Network

In addition to analyzing single telescopes, the simulation can be easily modified to analyze a collective group of telescopes. If any single telescope in the network can complete an observation, then the network as a whole can observe the event. There will be greater sky coverage as more telescopes are added to a network, therefore substantially increasing the observation probability. Networks of varying size and components will be simulated to determine the overall effect of having multiple telescopes searching for the same event. The simulations will also be used to decide which configurations provide the greatest observation probability. Data from these runs can then be used to build an optimum network when it comes time to perform the actual experiment after the completion of ALIGO and AVIRGO.

9 Acknowledgements

My mentor for this project was Dr. Eric Chassande-Mottin. He provided help and advice every step of the way and this project would have never gotten this far in two months without his oversight. My time spent at the Astroparticule et Cosmologie was funded by the National Science Foundation (NSF) through the University of Florida Gravitational Physics International REU Program. The weather function uses data provided by the Food and Agriculture Organization of the United Nations (FAO). The functions that directly calculated the Sun and Moon position were tested against observed Sun and Moon location data from the United States Naval Observatory (USNO). Moon illumination data was also used from USNO. All mathematical equations used in the functions were provided by the textbook "Astronomical Algorithms" by Jean Meeus.[10]

References

- [1] GariLynn Billingsley. Gravitational Wave Interferometry: How Does It Work. <http://www.ligo.caltech.edu/docs/P/P990027-00.pdf>.
- [2] MIT LIGO Laboratory CIT LIGO Laboratory. Laser Interferometer Gravitational Wave Observatory. <http://www.ligo.caltech.edu/>.
- [3] LIGO Data Analysis Software Working Group. How to Install LAL and LALApps Software. <https://www.lsc-group.phys.uwm.edu/daswg/docs/howto/lal-install.html>.

- [4] Denise Chow. 11 Most Amazing Astronomy Stories of 2011. <http://www.space.com/13980-top-science-astronomy-stories-2011.html>, December 2011.
- [5] Dr. Ken Ellrott. Instrumentation: Laser Interferometer Gravitational Wave Observatory (LIGO). <http://www.sr.bham.ac.uk/instrument/ligo.html>, January 2007.
- [6] Joan Centrella, Bernard Kelly, Jim Van Meter, John Baker, Robin Stebbins, and Robert Naeye. Computing Cosmic Cataclysms. *Scientific Discovery Through Advanced Computing Review*, 2012.
- [7] Alain Klotz. Determining the Best Locations on Earth for the French Ground Follow-up Telescope (GFT) of SVO. *CESR/OHP*, October 2007.
- [8] Laura Cadonati. Gravitational Wave Bursts and Multi-Messenger Astrophysics. In *Physics Colloquim - Duke University*, page 45. LIGO Scientific Collaboration and Virgo Collaboration, 2010.
- [9] R. Leemans and W. Cramer. The IIASA Database for Mean Monthly Values of Temperature, Precipitation, and Cloudiness on a Global Terrestrial Grid. <http://www.fao.org/WAICENT/FAOINFO/SUSTDEV/EIdirect/CLIMATE/EIsp0002.htm>.
- [10] Jean Meeus. *Astronomical Algorithms*. Willman-Bell Inc, 2nd edition, 1991.
- [11] Nature Photonics. Passing Gravitational Wave. <http://www.nature.com/nphoton/journal/v2/n10/images/nphoton.2008.186-f2.jpg>, 2008.
- [12] LIGO Scientific Collaboration. Introduction to Ligo and Gravitational Waves. <http://www.ligo.org/science/GW-Inspirals.php>.
- [13] LIGO Scientific Collaboration, Virgo Collaboration, and 817 Additional Authors. Implementation and Testing of the First Prompt Search for Gravitational Wave Transients with Electromagnetic Counterparts. *Astronomy and Astrophysics*, 2012.
- [14] Eric A. Smith. Shedding Light on Dark Energy. <http://atlantaapologist.org/rtb/index.php>, March 2012.
- [15] United States Naval Observatory. Rise, Set, and Twilight Definitions. <http://www.usno.navy.mil/USNO/astronomical-applications/astronomical-information-center/rise-set-twi-defs>.
- [16] United States Naval Observatory. Sun or Moon Altitude/Azimuth Table. <http://aa.usno.navy.mil/data/docs/AltAz.php>.